

Recent Developments on micro-SMES System Project at the University of Bologna

P.G. Albano, C.A. Borghi, M. Breschi, D. Casadei, A. Cristofolini, M. Fabbri, G. Grandi, P. La Cascia,
F. Negrini, U. Reggiani, P.L. Ribani, C. Rossi, G. Serra, A. Tani

Department of Electrical Engineering, University of Bologna, Viale Risorgimento 2, 40136 Bologna, Italy

Abstract - The micro-SMES (Superconducting Magnetic Energy Storage system) project of the University of Bologna, begun in September 1997, is aimed to design and realize a 200 kJ/ 75 kW prototype. The project should be completed within the end of 2001. Two main subprojects are carried on: the former concerns the design of the SC (Superconducting Coil) and the cryogenic system. The latter is related to the development of the PCS (Power Conditioning System). This paper presents the configuration of the designed Superconducting Magnet and the structure of the Power Conditioning System. The principle of operation will be also analyzed with reference to the control of the energy flow between the components of the PCS. Numerical and experimental results will be shown to demonstrate the effectiveness of the PCS to reduce flicker phenomena and to compensate harmonic current components and reactive power.

I. INTRODUCTION

The first task of the SM design is the determination of the geometry of the coils for a fixed magnetic energy and a specified superconducting technology. To reduce the costs of the device, the volume of the superconductor wire should be reduced as much as possible. Moreover, to have a compact and manageable system, the whole device volume has to be minimum. The two goals can not be fulfilled at the same time. Thus, a multiobjective minimization problem arises. The magnetic energy, the stray field, and the superconductor characteristics are taken as constraints. A comparison between the axisymmetric coil configuration and a toroidal one has been done, and the reference model is now the one/two coils axisymmetric device. For what concerns the design of the cryogenic system, it is now under development, and a reference configuration has been identified to be a pool-boiling magnet with recondensation of helium vapor by means of a cryo-cooler [1], [2].

A Power Conditioning System (PCS) which can be utilized for the compensation of non-linear and pulsating loads is analyzed in this paper. In order to provide the expected features, the PCS considered in this paper has a topology including a voltage source inverter and a two-quadrant current chopper, as represented in Fig. 1. The two converters are decoupled by a dc-link. The SC is characterized by a relatively large inductance and behaves as a constant dc current source. The chopper operates in order to control the capacitor voltage of the dc-link. The Voltage Source Inverter (VSI) acts as interface between the dc-link and the ac power supply, controlling the power flowing through the series ac-link inductors. The whole PCS is based on the use of state of the art power electronics such as IGBTs. Thanks to their switching capabilities a PWM modulation technique can be carried out for the VSI inverter reducing the harmonic content at the switching frequency and improving the current control capability [3]. This converter structure is able to control reactive power transferred to the mains, and to reduce the flicker phenomena, moreover it has the topology of a shunt active filter yielding to the inherent capability to perform the load harmonic current compensation.

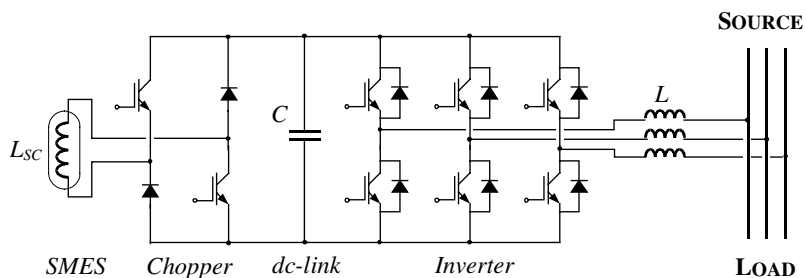


Fig. 1 Scheme of the PCS structure

	Coil 1	Coil 2
Inner radius	0.155 m	0.508 m
Outer radius	0.189 m	0.510 m
Height	0.166 m	0.338 m
Number of turns	7513	900
Maximum magnetic induction	5.466 T	4.857 T
Maximum normal stress (without structural material)	47.98 MN/m ²	15.44 MN/m ²

Table - specifications of the reference configuration

A complete control system for the PCS which is able to satisfy, at the same time, the requirements of shunt active filters and power conditioners is presented. The control system is composed of three independent regulators which are designed in order to keep under control the SC energy, the dc-link voltage, and the VSI ac currents [4]. A detailed analysis is carried out for each regulator, determining

the transfer function and showing the influence of the regulator parameters. Then a complete control system suitable to be implemented on a Digital Signal Processor (DSP) has been developed. Numerical simulations have been performed considering a linear R-L load, a non-linear full bridge diode rectifier load, and a pulsating load. The results obtained show that the proposed control system is able to behave as power conditioner and active filter at the same time.

II. SUPERCONDUCTING MAGNET DESIGN

In the subproject related to the design of the superconducting magnet some methodologies for the optimized electromagnetic design of superconducting coils have been developed. It has been chosen a reference configuration constituted by two series connected coaxial solenoids, wound in opposite directions. This choice minimizes the stray field thanks to active shielding and it is utilizable for an industrial size device too. A single strand, copper stabilized, NbTi cable has been considered for the design of the prototype. It is the same superconducting wire utilized for LHC (Large Hadron Collider) accelerators and thus readily available.

The reference configuration has been achieved minimizing the volume of the superconductor, and thus the cost of the device, constraining the stray field to values under 0.5 mT. The overall dimension, defined as the region with magnetic field over 0.5 mT, has been fixed in a cylinder 3.0 m high and with a radius of 1.5 m. The carried out choice is the compromise solution between the minimum size and the minimum cost option (see Figs. 1 - 3). Even if the size of the reference configuration is not optimized, it remains in the limits for an industrial use. In Table 1 are listed the main data of the electromagnetic reference configuration.

The correct working condition of the superconductive part is ensured by the cooling system that has to keep the coil temperature at 4.2 K. The heat produced in the coil, mainly due to AC losses, and in the current leads, due to Joule effect, must be removed. The cryogenic system has been identified to be a pool-cooling type using liquid helium, with recondensation of helium vapor by means of a “Gifford - McMahon” cryo-cooler. The system needs a starting filling of liquid helium, but it doesn’t require further maintenance except for monitoring the liquid level and the temperature. The cryo-cooler system consists of three main components. The component that is incorporated in the cryostat is the “cold head”. This is a two-stage device with the first stage being used to cool a thermal shield to about 40 K and the second stage being used to recondense any evaporated helium gas.

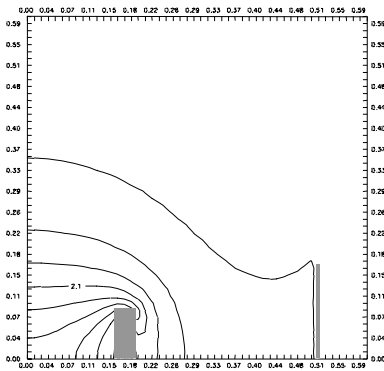


Fig. 2a – Lines of constant z-component of the magnetic field density for the reference configuration.

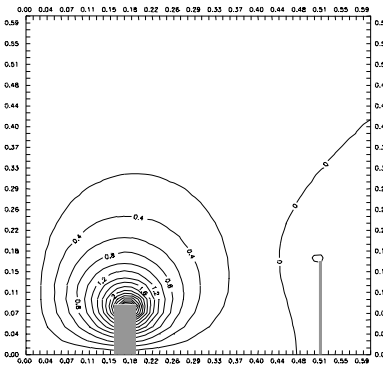


Fig. 2b – Lines of constant r-component of the magnetic field density for the reference configuration.

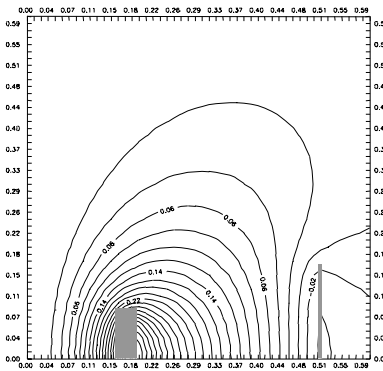


Fig. 2c – Lines of magnetic flux density for the reference configuration.

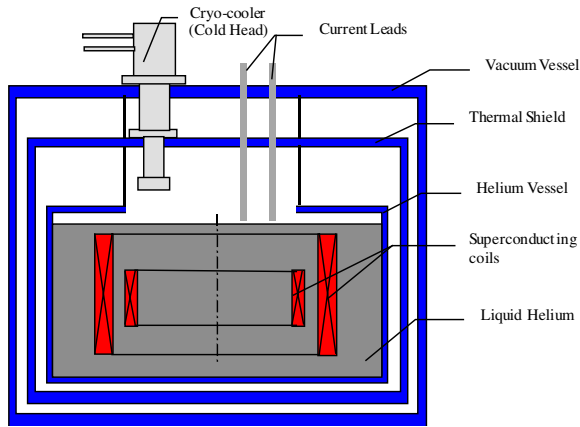


Fig. 3 – Scheme of the main features of recondensing cryostat

The cryostat will contain a gas buffer volume above the liquid helium. During ramping of the magnet, the instantaneous heat load will exceed the cooling power of the cold head. The gas evaporated will be stored in the buffer volume at slightly elevated pressure and will be gradually recondensed over several hours. Providing the next experiment is not run until the helium vessel is back at its working pressure, it should be possible to make the system truly loss-less as far as helium consumption is concerned. The current leads (hybrid type, high temperature superconductor) pass through the vacuum vessel, the thermal shield and the helium vessel and connect the superconducting coil to the power conditioning system. A sketch of the device is shown in Fig. 3.

III. POWER CONDITIONING SYSTEM PCS

III - 1 PRINCIPLE OF OPERATION

For the analytical developments, the three-phase quantities are represented by space vectors in the stationary reference frame dq . The three-phase PLL allows to extract the vector \bar{v}_s which represents only the fundamental positive sequence of the utility voltage [5].

The behavior of the PCS is determined by three closed-loop regulators, as represented in the block diagram of Fig. 4. The first regulator controls the VSI ac currents, the second one the dc-link voltage and the third one the SC energy.

The ac-current regulator performs the basic principle of the control system that is to impose sinusoidal source currents in phase with the corresponding fundamental positive sequence of the source voltages. Then, the reference value of the source current is represented by the current vector \bar{i}_s^* in phase with the source voltage \bar{v}_s . The source current magnitude I_s^* is obtained by the regulator R_1 , acting on the instantaneous error between the reference value of the SC energy E_{SC}^* and its actual value E_{SC} , being $E_{SC} = \frac{1}{2} L_{SC} I_{SC}^2$. The regulator R_1 operates in order to keep

the SC energy close to its reference value.

The two-quadrant chopper performs a PWM current control by the regulator R_2 . In this way the dc-link voltage V_C is kept close to its reference value V_C^* and the energy stored in the capacitor is nearly constant. Thus, the active power is flowing directly from the supply to the SMES (with exception of the switch and inductor losses).

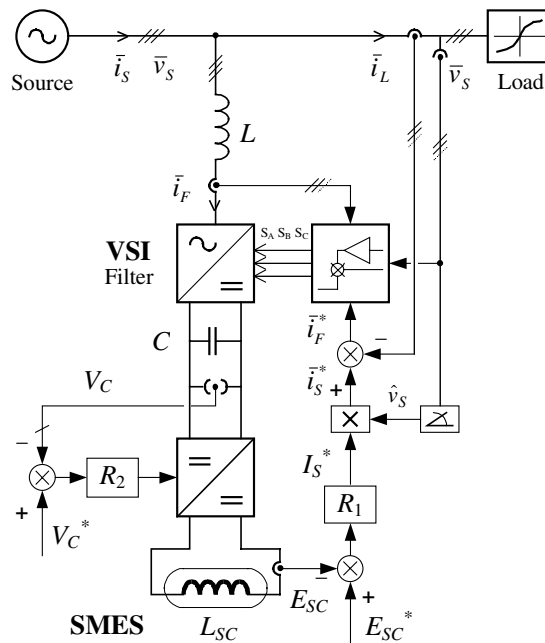


Fig. 4. Block diagram of the PCS control scheme

III.2 ANALYSIS OF THE CONTROL LOOPS

The power conditioning system analyzed in this paper should be designed in order to satisfy the requirements related to various tasks, in different frequency ranges:

- reduction of flicker ($\ll 50$ Hz)
- current harmonic compensation ($\gg 50$ Hz)
- reactive power compensation (50-60 Hz)

The performance of the PCS for the reduction of flicker is determined by the regulator which performs the SC energy storage control. Transient changes in the instantaneous power absorbed by the load generates voltage fluctuations across the dc capacitor. The dc-link voltage control loop should smooth voltage fluctuations within few cycle periods

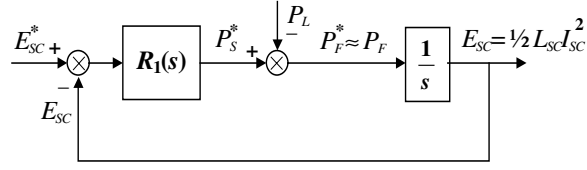


Fig. 5. Block diagram of the SC energy control loop

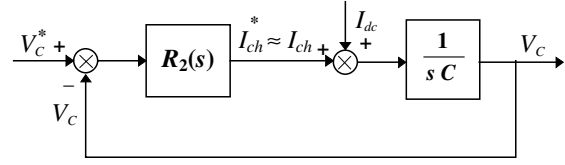


Fig. 6. Block diagram of the dc-link voltage control loop

(i.e., tens of ms). The dynamic behavior of the active filter, is determined by the time response of the ac current control loop, which must be fast enough to track the reference current waveforms closely (i.e., fractions of ms). In order to compensate reactive power and current harmonics of non-linear loads, the PCS must operate as an active filter. Then, the three regulators have different features, requiring quite different time responses. Thus, they can be designed as three independent control loops.

III.2.1 SC Energy Control Loop

The dynamic behavior of the SC energy control loop is investigated with reference to the block diagram of Fig. 5. The input of the regulator R_1 is the error of the SC stored energy, the output is the reference value of the source power P_S^* defined as $P_S^* = V_s I_s^*$. The reference value of the power absorbed by the filter P_F^* is calculated by subtracting the load power P_L to P_S^* . Assuming that the PWM inverter is able to generate the reference power at each cycle period, yields $P_F = P_F^*$. This instantaneous power represents the total power flowing from the supply to the PCS. Neglecting the rate of change of the magnetic energy in the link inductors, P_F represents the input power to the VSI. Furthermore, the dc-link voltage can be considered constant, being the dc-link control loop faster than the SC energy control loop. As a consequence, neglecting the losses of the two converters, the energy stored in the SC (E_{sc}) is given by the time integral of P_F .

Under these assumptions, the following expression can be derived from the block diagram represented in Fig. 5

$$E_{sc} = \frac{R_1(s)}{s + R_1(s)} E_{sc}^* - \frac{1}{s + R_1(s)} P_L \quad (1)$$

As (1) shows, the load power P_L represents a perturbation in the SC energy control loop. The effect of this perturbation is determined by the type of regulator, i.e., by the expression $R_1(s)$.

The aim of this control loop is to smooth the load power fluctuation which determine the flicker phenomena. The relationship between the load power and the source power is expressed by

$$P_S = \frac{R_1(s)}{s + R_1(s)} P_L \quad (2)$$

III.2.2 DC-Link Voltage Control Loop

The analysis of the dc-link voltage regulator is carried out with reference to the control scheme represented in Fig. 4.

The input of the regulator R_2 is the dc-link voltage error, the output is the reference value of the chopper current I_{ch}^* .

In this case, the perturbation is represented by the dc-side current of the VSI, I_{dc} . From the block diagram of Fig. 4, the following transfer function can be obtained

$$V_c = \frac{R_2(s)}{sC + R_2(s)} V_c^* + \frac{1}{sC + R_2(s)} I_{dc} \cdot \quad (3)$$

In this case, the dc-link voltage must be regulated to its reference value to ensure a correct operation of the inverter.

The choice for two PI regulators as $R_1(s)$ and $R_2(s)$ allows to obtain that load power does not introduce steady-state error in the SC stored energy, and the dc-side current of the VSI does not introduce steady-state error in the dc-link voltage.

III.2.3 AC Currents Control Loop

The ac-side inverter currents are controlled according to the block diagram shown in Fig. 7. The inverter reference voltage is determined on the basis of the voltage equation written across the ac-link inductor

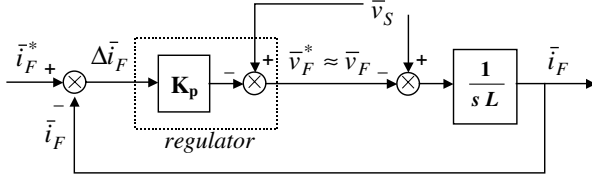


Fig. 7. Block diagram of the filter ac current control loop

following equation is obtained

$$\bar{i}_F = \frac{1}{1 + \tau s} \bar{i}_F^*, \text{ where } \tau = \frac{L}{K_p}. \quad (5)$$

Eq. 5 shows that the response of the ac current loop is represented by a simple first order low-pass filter. As it could be expected, the time constant τ is proportional to the ac-link inductance L , but the effect of this inductance can be compensated by selecting a suitable value for K_p . However, the dynamic performance of the control loop cannot be improved indefinitely, being the inverter output voltage limited by the dc-link voltage.

III.3 SIMULATION RESULTS

The behavior of the power conditioner control system presented in Section III.2 has been analyzed in detail by numerical simulations carried out in Simulink environment.

The simulations are related to a power conditioning system characterized by the following data: Rated energy in the SC coil $E_{SC}^* = 150$ KJ; Rated energy in the capacitor bank $E_C^* = 980$ J; Maximum load power $P_L = 30$ KW.

Figs. 8,9,10 show the behavior of the PCS to 100% load variations. Fig. 8 shows the system response during the switch on of load, Fig. 9 and 10 illustrate the system response when a pulsating load is connected to the mains. The load pulsation frequency is 0.01 Hz in Fig. 9 and 5 Hz in Fig. 10. These results are related to steady state initial conditions, being the SC energy and capacitor voltage close to their rated values. During the load switching the maximum energy variation in the capacitor is $\approx 5\%$, whereas in the SC coil is $\approx 3\%$ of the rated value (see Figs. 8-b,c and Figs. 9-b,c). These small variations of the energy make it possible to of the rated energy allow to keep the voltage across the dc capacitor inside a band that guarantees the correct operation of the inverter, and the energy in the SC at a value that guarantees the operation of the system as UPS for few seconds. Fig. 10-a,b,c show the system capability to compensate flicker phenomena. The mean value of the source power corresponds to the power absorbed by the load. Figs. 10-b,c show small energy variations in the capacitor and in the SC coil around their rated value.

III. 4 EXPERIMENTAL SYSTEM

Being, at this stage of the project development, the Superconductive Coil not yet available, only the behaviour of

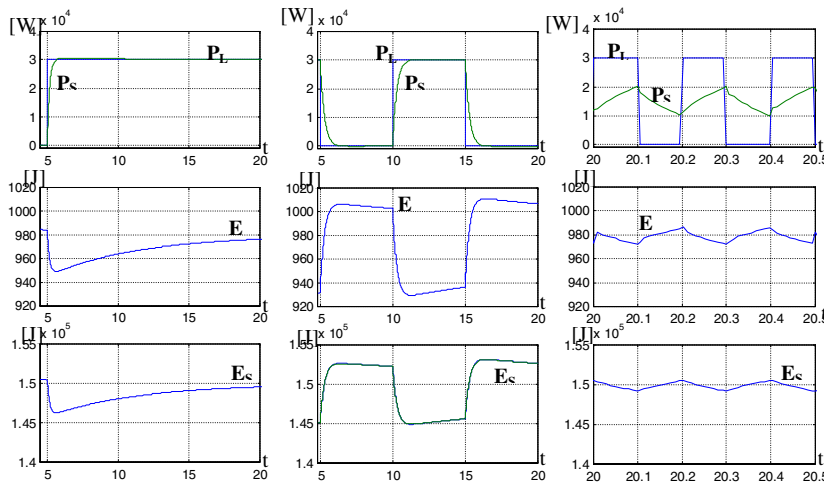


Fig. 8-a,b,c Switch on of the load

Fig. 9-a,b,c Switch on and off of the load

Fig. 10-a,b,c Pulsating load. Frequency 5 Hz

the PCS as active filter is investigated. To validate the numerical simulations, the control system has been digitally implemented on a PPC 333 MHz DSP based board.

Fig. 11 shows the block diagram of the PCS used for the experimental tests. The topology of the experimental PCS is simpler than the scheme shown in Fig.4 because the dc/dc converter is not used. In this configuration the PCS is able to reduce the harmonic currents and to compensate the reactive power and

$$\bar{v}_F^* = \bar{v}_S - K_p \Delta \bar{i}_F. \quad (4)$$

In this case, the control is performed by a feed-forward compensation of the source voltage and by a simple proportional gain. With reference to Fig. 7, it is possible to determine the transfer function of the closed loop system.

If we assume that the PWM inverter is able to generate the reference voltage at each cycle period, the

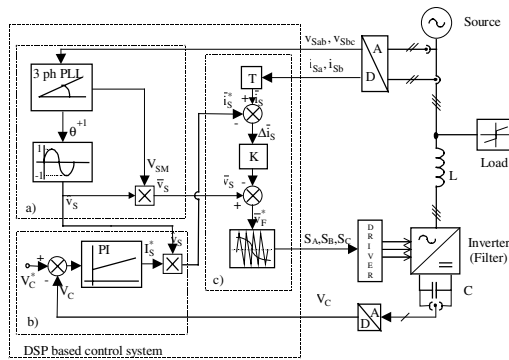
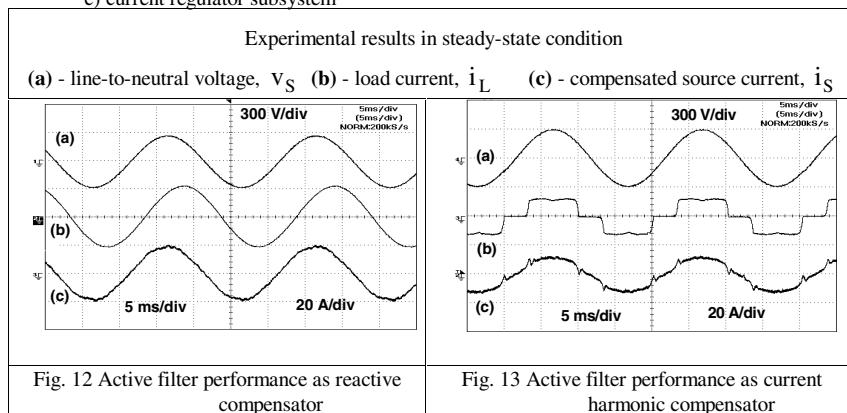


Fig. 11. Block diagram of the active filter used for experimental tests
a) source voltage identification subsystem
b) dc voltage regulator subsystem
c) current regulator subsystem



the source current, with exception of the high order harmonics due to the fast current commutations.

IV. CONCLUSIONS

A control scheme for Power Conditioning Systems, in which a SMES is employed for energy storage has been analyzed in this paper.

The main feature of the PCS structure combined with the proposed control system is the possibility to solve several power quality problems. This system is able to compensate reactive power and current harmonics due to linear or non-linear loads. The availability of energy stored in the Superconductive Coil gives the ability to smooth flicker phenomena. The configuration of the system allows further development like the possibility to use the system as UPS during short time utility faults.

The control scheme has been tested in different operating conditions by numerical simulations. In this way, the dynamic behavior of the whole system has been verified with good accuracy. The proposed control scheme is quite simple and it has been implemented in the demonstrative PCS realized at the University of Bologna.

REFERENCES

- [1] C.A. Borghi, M. Fabbri, P.L. Ribani, "Design Optimization of a Microsuperconducting magnetic Energy Storage System", *IEEE Trans. Magn.*, vol. 35, pp. 4275-4284, September 1999.
- [2] M. Fabbri, F. Negrini, P.L. Ribani, "Optimized Magnetic Design of a High Temperature micro-SMES", *Int. J. of Modern Physics B*, vol. 13, n. 9 & 10, pp. 1351-1356, 1999.
- [3] D. Casadei, G. Grandi, U. Reggiani, C. Rossi, "Active Power Filter with Minimum Measurement Requirements", *IEEE, APEC '99 Conf. Proc.*
- [4] D. Casadei, G. Grandi, U. Reggiani, G. Serra, "Analysis of a Power Conditioning System for Superconductive Magnetic Energy Storage", - ISIE 98, Pretoria (SA), July 1998.
- [5] D. Casadei, G. Grandi, C. Rossi, "Effects of Supply Voltage non-Idealities on the Behavior of an Active Power Conditioner for Cogeneration Systems", - PESC 00, Irland, June 2000.

the unbalancing of the load. The IGBT VSI is shunt-connected to the 220 V, 50 Hz utility by means of a 2 mH, 3-phase ac-link inductor. The dc-link capacitance is 1000 µF and the reference dc-link voltage is 450 V.

In this experimental system, the generation of the reference source current magnitude I_S^* is realized in a simplest way with respect of that shown in Fig. 4. Being this system without the SC coil, the generation of I_S^* is obtained from the dc link voltage regulator that keep the voltage across the capacitance close to its reference.

The active power filter prototype has been firstly used to compensate the reactive power of a linear R-L load ($\cos \phi = 0.8$).

The results obtained are shown in Fig. 12. As expected, the

reactive power is compensated and the resulting source current is almost sinusoidal and in phase with the corresponding line-to-neutral voltage.

The harmonic compensation capability of the active filter has been tested connecting a three phase full bridge diode rectifier (non-linear load) to the mains. The results are shown in Fig. 13. The load current harmonics disappear in